ELSEVIER

Carbohydrate Polymers 46 (2001) 7–18

Carbohydrate Polymers

www.elsevier.com/locate/carbpol

A proton NMR relaxation study of the gelatinisation and acid hydrolysis of native potato starch

H.-R. Tang, A. Brun, B. Hills*

Institute of Food Research, Norwich Research Park, Colney, Norwich NR4 7UA, UK

Accepted 6 July 2000

Abstract

The effect of acid hydrolysis (Lintnerisation) and the thermal gelatinisation on the dynamic state of starch and the microscopic distribution of water within native potato starch granules is investigated with proton NMR relaxometry. The NMR relaxation data show several dynamic states of the amylose and amylopectin chains and clearly identify the melting transition during thermal processing. The Lintnerisation process is found to follow first-order kinetics and to shift and broaden the melting transition. The unique value of NMR relaxometry for monitoring the processing response of starch granules is discussed. © 2001 Elsevier Science Ltd. All rights reserved.

Keywords: Starch; NMR; Gelatinisation; Lintnerisation

1. Introduction

The structure of native starch granules has been studied for many years with a variety of microscopic and scattering techniques, including SAXS and WAXS. While the details of granule structure remain a matter of debate, the composite model of amorphous growth rings and alternating semi-crystalline lamellae is now generally recognised (Blanshard, 1987; Gallant, Bouchet, & Baldwin, 1997). What the models of granule structure do not show is the microscopic distribution of water within the granule or the changing dynamic state of the amylose and amylopectin. These factors are expected to play a critical role in determining the response of the granule to processing operations such as thermal gelatinisation and acid hydrolysis (Lintnerisation). For example, the local concentration of water in different parts of the granule will affect the local amylose or amylopectin glass transition temperature and therefore the melting temperature of each granule compartment and the water and amylose diffusion rates.

Our ignorance about local water distribution and the changing dynamic state of the starch components makes it impossible at the present time to predict quantitatively the effect of chemically, genetically or enzymatically modifying the granule on its subsequent response to processing. Part of the problem is the lack of suitable physical methods for monitoring, in real time, the changing microscopic distribution, and dynamic state of the starch and water components during processing. Small angle neutron scattering (SANS) is an exception to this statement because it has been used to probe water distribution inside waxy maize granules during gelatinisation (Donald et al., 1997). However, interpretation of the SANS data relies on simplified models of granule microstructure and the technique is not widely available. DSC studies of the gelatinisation of potato starch granules as a function of water content were reported as early as 1979 by Donovan. At intermediate water contents two endothermic transitions were observed, labelled the G and M1 endograms. The G endotherm has been interpreted as the transition of the amorphous (amylose rich) regions of the granule from the glass to rubbery aqueous gel. The M1 endotherm has been assigned to the melting of the crystalline (amylopectin rich) regions of the granule (Blanshard, 1987; Muhr, Blanshard, & Bates, 1984). If the water content is increased the G peak increases in amplitude as more swelling is permitted and the M1 peak moves to lower temperatures and eventually merges with the G peak. This is taken to show that at high water contents the swelling and mobilisation of the amylose-rich amorphous region destabilises the crystalline amylopectin-rich region and facilitates its melting.

Acid hydrolysis (Lintnerisation) is another useful method for exploring structure–function relationships by selectively hydrolysing different parts of the granule and observing the subsequent effect on gelatinisation. The observation that at a water content for which there were both G and M1

* Corresponding author. Tel.: +44-1603-255000; fax: +44-1603-507723.

E-mail address: brian.hills@bbsrc.ac.uk (B. Hills).

PII: S0144-8617(00)00265-4

endotherms, prolonged acid treatment leaves only the M1 peak supports the idea that acid preferentially hydrolyses the amylose rich amorphous regions of the granule (Jacobs, Eerlingen, Rousen, Colonna, & Delcour, 1998). The residues from acid hydrolysis (Lintnerised starches) have also been examined by scattering techniques including wide-angle X-ray scattering (WAXS), small-angle light scattering (SALS), small-angle neutron scattering (SANS) and small-angle X-ray scattering (SAXS) (Jenkins & Donald, 1997, 1998). The results confirm that the amorphous regions in the granule are preferentially hydrolysed and that this has a strong influence on the subsequent gelatinisation behaviour of the starch. This agrees with earlier work of Robin, Mercier, Charbonniere, & Guilbot (1974, 1975) who observed a two-stage hydrolysis process, an initial fast stage (0–8 days) postulated to arise from the hydrolysis of the amylose rich, amorphous regions; followed by a slower stage (8–40 + days), attributed to hydrolysis of the more crystalline, amylopectin-rich, regions.

Further insight into structure–function relations can be obtained by examining the structure and behaviour of the composite starch gels obtained by partial gelatinisation of starch with different water contents. Light microscopy has shown that the composite consists of an amylose gel network containing granule "ghosts" of amylopectin embedded with it. The "amylopectin ghosts" appear as hollow spheres containing amylose gel (Hermansson, Kidman, & Svegmark, 1995). It appears, therefore, that the M1 endotherm does not correspond to complete destruction of the amylopectin structure but only to partial plasticisation and gelation. There is no evidence that substantial amounts of amylopectin are released from the granule. (Morris, 1990).

NMR is undoubtedly the technique of choice for studying the dynamic state of biopolymers and water so it is surprising that relatively little NMR relaxometry has been done on starch gelatinisation and Lintnerisation. In a recent paper (Tang & Hills, 2000) we explored the relationship between water distribution and granule microstructure in native, unprocessed granules using a variety of proton and deuterium NMR techniques. By monitoring the temperature dependence of the distribution of water proton transverse relaxation times for a packed bed of potato starch granules three distinct water populations could be identified. These were assigned to a thin film of bulk water between the packed granules; to water in the amorphous growth rings and to water in the semi-crystalline lamellae. The last two populations were found to be in fast exchange at room temperature but entered the slow exchange regime below 277 K with a diffusive exchange lifetime of approximately 1 ms. In addition, a fourth population of orientationally ordered, intra-granular water was identified by its characteristic 1 kHz wide splitting in the deuterium spectrum of granules soaked in D_2O. This was assigned to water inside the hexagonal channels of B-type amylopectin crystals in the semi-crystalline lamellae. This "channel water" did not exchange with the other water populations on the NMR measurement timescale.

In this paper we use the same NMR methods to explore the effects of gelatinisation and Lintnerisation on the dynamic state of the starch and on the microscopic compartmentation of the water. No attempt is made in this paper to undertake comparative studies on the effects of different types of starches, water contents or pre-processing (annealing) treatments. Instead we focus on a water-saturated bed of packed native potato starch granules and try to relate the effects of gelatinisation and Lintnerisation to changes in the NMR relaxation behaviour. In future papers these data will be used to compare the effects of modifying granule structure, pre-processing conditions and water content on the gelation and Lintnerisation kinetics.

2. Experimental

NMR water proton transverse relaxation times were acquired on a Bruker MSL100 spectrometer operating at a resonance frequency of 100.13 MHz. A solenoid RF coil was used with horizontal, 5 mm internal diameter tubes. This gave short 90° pulses of 1–2 μs. Free induction decays (FID) were determined with a single 90° pulse of 2 μs duration and a dwell time of 4 μs. Transverse relaxation times were measured with the Carr–Purcell–Meiboom–Gill (CPMG) pulse sequence used with a 90–180° pulse spacing of 150 μs and full phase cycling. A recycle delay of 10–15 s was used to avoid saturation effects and 48–64 acquisitions were accumulated. The FID and CPMG echo decay envelopes were analysed as a continuous distribution of exponentials with Resonance Instruments WINDXP software. To avoid over-processing of data, the regularisation parameter in this inversion was determined from the amount of noise in the baseline. Temperatures were thermostated in the usual way using a liquid nitrogen evaporator.

NMR water deuterium spectra were acquired on a Bruker MSL300 spectrometer operating at a deuterium resonance frequency of 46 MHz with a 90° pulse of 2.1–2.6 μs. The quadrupolar echo pulse sequence was used with a delay of 40 μs and a dwell time of 4 μs. Deuterium exchanged starch granules were prepared by suspending the granules in excess D_2O, allowing them to settle under gravity, and replacing the supernatant with pure D_2O. This cycle was repeated three times.

Native potato starch granules were subjected to the Lintnerisation process for controlled periods up to 32 days. After treatment, the granules were washed several times with distilled water and examined as a water-saturated packed bed on a Bruker MSL100 spectrometer. The absence of residual acid in the washed, packed bed was checked by measuring its pH. Attempts to examine the hydrolysis in the NMR tube "in situ" without washing failed because the high ionic strength of the acid created difficulties with NMR probe tuning. All experiments used potato starch purchased from BDH and used without further treatment.

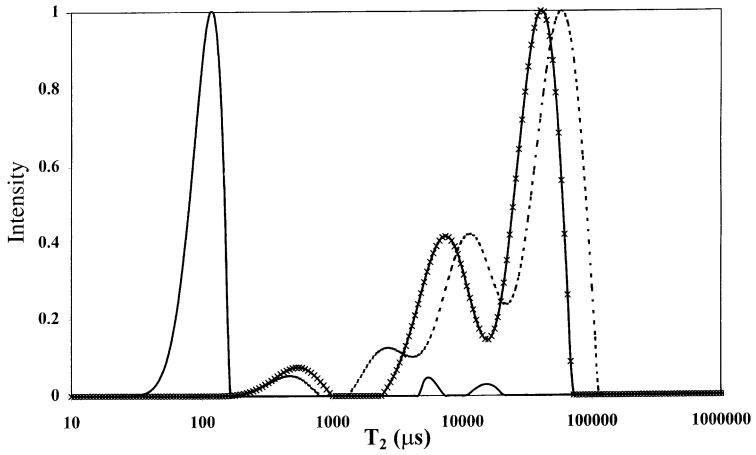

Fig. 1. The distribution of water proton transverse relaxation times measured with the CPMG pulse sequence at the indicated temperatures for a water-saturated packed bed of native potato starch granules.

Recrystallised Spherulite (DP = 22) were supplied by Dr S. Ring of the IFR.

3. Results

3.1. The microscopic compartmentation of water in a packed bed of native granules

Fig. 1 shows the distribution of water proton transverse relaxation times in a water-saturated packed bed of native potato starch granules at three temperatures, 270, 277 and 300 K. Four relaxation time peaks can be distinguished at 277 K and, in a previous paper, these were assigned to four water compartments (Tang & Hills, 2000). The longest relaxation time peak arises from water outside the granules; the next two shorter relaxation time peaks observed at 277 K arise from slowly exchanging water in the amorphous growth rings and semi-crystalline lamellae. Finally, the shortest relaxation time peak at about 200 μs has been assigned to water in the hexagonal channels of B-type amylopectin crystals (Tang & Hills, 2000), though contributions from mobile starch CH protons cannot be ruled out. Raising the temperature to 300 K causes the merging of the

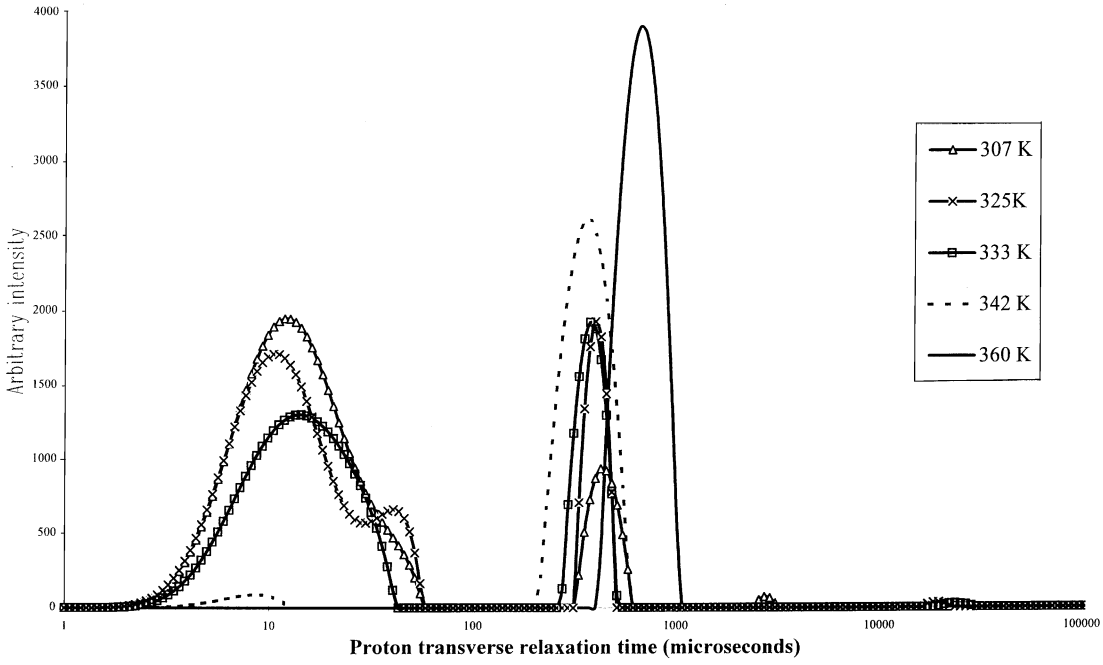

Fig. 2. The distribution of transverse relaxation times for non-exchanging starch protons measured with the Free Induction Decay at the indicated temperatures for a packed bed of native potato starch granules in D_2O.

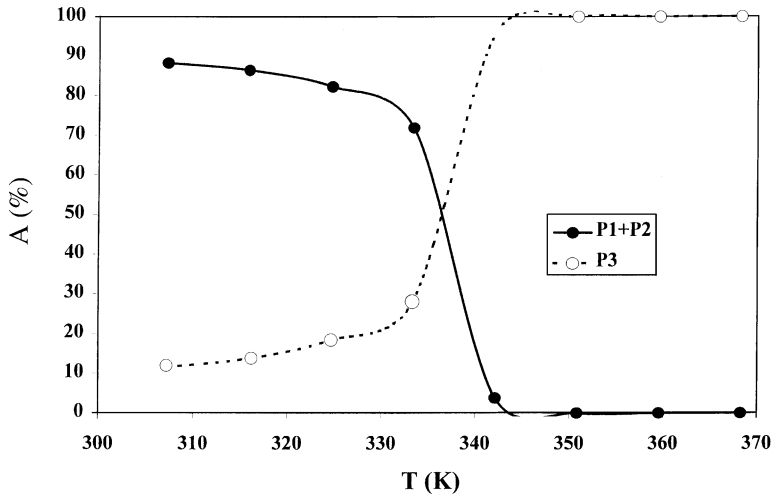

Fig. 3. The temperature dependence of the relative percentage area of the longest relaxation time peak (labelled P3) in Fig. 2. P1 and P2 refer to the less well-resolved short relaxation time peaks in Fig. 2. Additional temperatures not plotted in Fig. 2 have been included.

two middle peaks because of fast diffusion of water between the amorphous growth rings and semi-crystalline lamellae. Freezing at 270 K removes most of the water proton signal because ice has a transverse relaxation time of just a few microseconds. The new peak at about 100 μs presumably corresponds to starch CH protons and also to residual signal from small amounts of non-freezing water hydrating the starch chains.

These results show that NMR relaxometry is a potentially powerful tool for probing the changing microscopic distribution of water during starch granule processing. Two processing treatments are of particular importance and these are thermal gelatinisation and Lintnerisation:

3.2. The effect of thermal gelatinisation on the starch chain mobility

The effect of progressively heating a water-saturated, packed suspension of native potato starch granules was followed inside the NMR probe. In this experiment water (H_2O) was replaced by D_2O so that only the changing starch chain dynamics is observed via the proton transverse relaxation of the amylose and amylopectin chains. The dynamics were monitored on a short timescale of 4–1000 μs using the FID and also on a longer relaxation timescale of 1 ms–1 s using the CPMG pulse sequence. Fig. 2 shows the results for the FID and shows three main relaxation time components

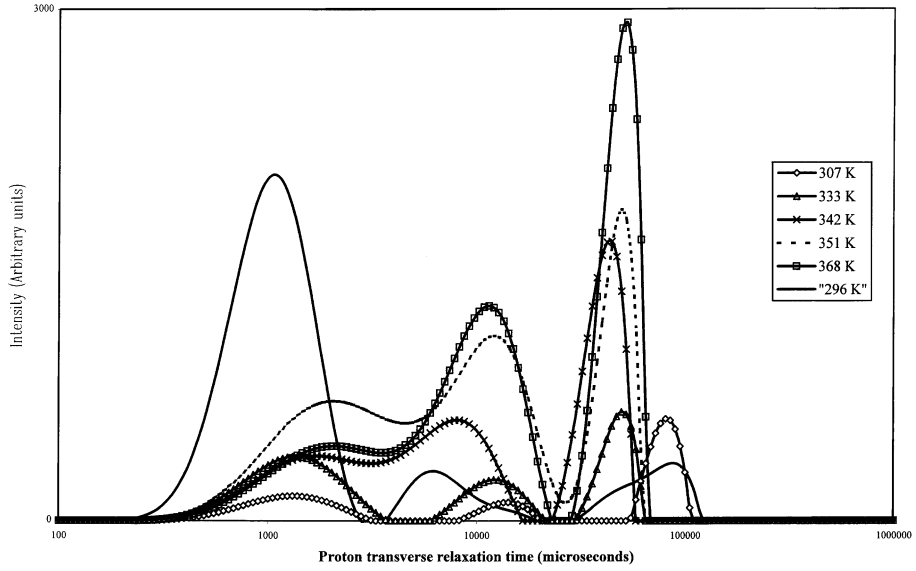

Fig. 4. The distribution of transverse relaxation times for non-exchanging starch protons measured with the CPMG sequence at the indicated temperatures for a packed bed of native potato starch granules in D_2O. The curve labelled "296 K" is the result after cooling the sample after heating to 368 K.

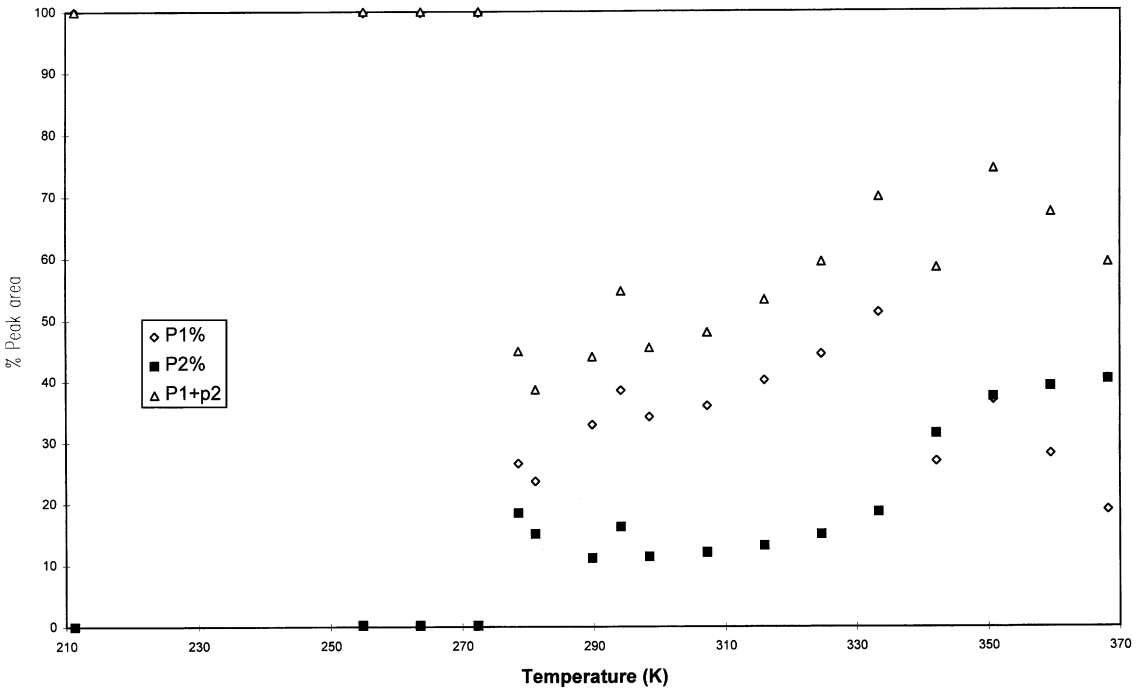

Fig. 5. The temperature dependence of the relative percentage area of the longest relaxation time peak (labelled P3) in Fig. 2. P1 and P2 refer to the two short relaxation time peaks in Fig. 4. Additional temperatures not plotted in Fig. 4 have been included.

at ca. 10, 50 and 500–700 μs, depending on the temperature, though the middle component at 50 μs is not always well resolved in the relaxation time distribution. It is worth noting that although one might expect the solid part of the FID to have a significant Gaussian component the raw data at 295 K for the water-saturated bed of fully swollen granules shows that the FID is reasonably well represented as a monotonic multiple exponential decay with no evidence of a solid-like dipolar dip.

It is difficult to assign the three relaxation peaks in Fig. 2 to particular chain components. The shortest relaxation time peak at 10 μs probably corresponds to rigid amylopectin in the semi-crystalline lamellae. The longest relaxation time peak at ca. 500–700 μs then corresponds to more mobile amylopectin in the amorphous regions of the granule. The same peaks are observed in waxy maize starch in D_2O which lacks amylose, so it is necessary to assign them to the amylopectin component. As the temperature is slowly raised the plasticisation of the amylopectin is seen in the increase in the relative peak area of the longest peak at ca. 500–700 μs relative to the other peaks and this is plotted in Fig. 3. It is obvious that there is a transition temperature at about 335 K and this is associated with the melting or plasticisation of the amylopectin component.

Fig. 4 shows the behaviour on the longer timescale of 100 μs–1 s probed by the CPMG sequence. The relaxation peak at ca. 1 ms is probably the same as the longest peak at 500 μs seen in the FID and therefore arises from amylopectin in the amorphous regions of the semi-crystalline lamellae. It is well known that the slowly decaying part of the FID measures T_2^* which, because of susceptibility effects and off-resonance components is always slightly shorter than the true T_2 measured by the CPMG sequence. However, there are also two longer relaxation time peaks in the CPMG relaxation spectrum at ca. 20 and 80 ms. The peak at 20 ms is also observed in the corresponding CPMG relaxation time spectrum of waxy maize starch, so this also must be assigned to mobile amylopectin CH protons, presumably in the most mobile regions of the amorphous growth rings. However, the longest relaxation time peak at ca. 80 ms in Fig. 4 can be safely assigned to amylose CH protons because it is not seen in the corresponding waxy maize relaxation spectrum.

As the temperature is raised the relative area of the longest relaxation time peak at 500–700 μs in Fig. 2, and assigned to amylopectin in the amorphous part of the semi-crystalline lamellae (and labelled P3 in Fig. 3), progressively increases as the amylopectin is progressively plasticised. A transition temperature of about 335 K is clearly seen in the data. The same transition can be seen in Fig. 5 which plots the areas from the corresponding CPMG data in Fig. 4. The plasticisation of the amylopectin at ca. 335 K is seen in the drop in the relative area of the peak at 1 ms (labelled P1 in Fig. 5).

Fig. 4 also shows that the area of the amylose peak at ca. 80 ms also increases quite dramatically above 335 K, presumably as the amylose plasticises and gelatinises.

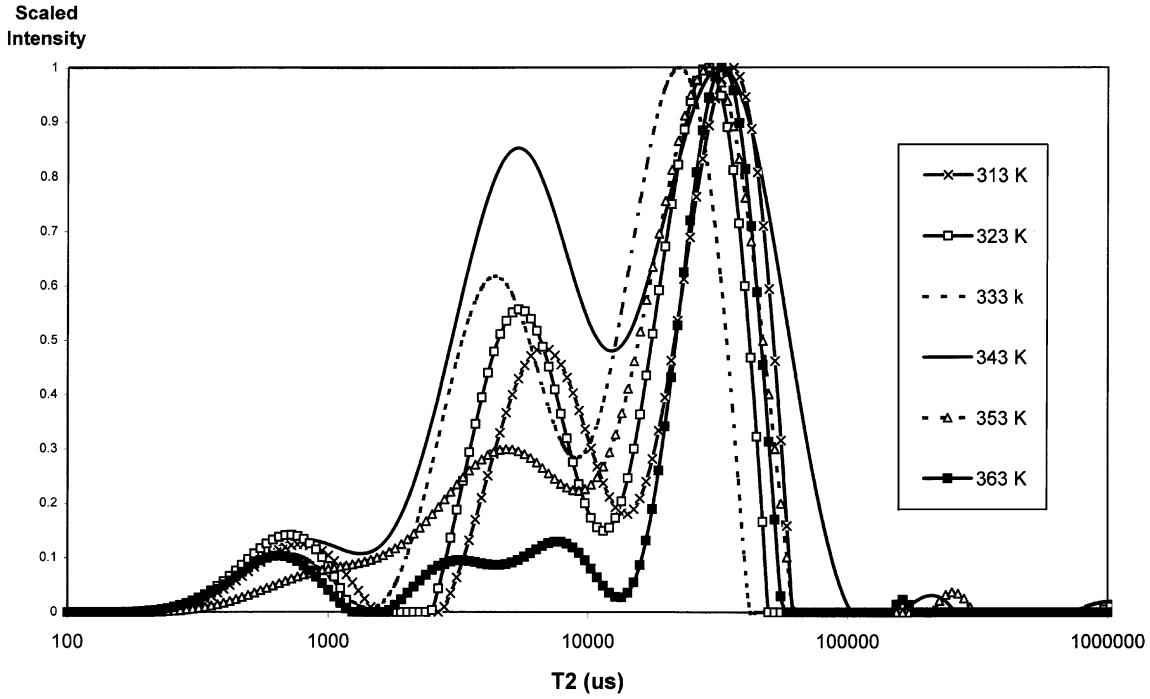

Fig. 6. The distribution of water proton transverse relaxation times measured with the CPMG sequence at the indicated temperatures for a packed bed of native potato starch granules in H_2O.

This is seen in Fig. 5 as a drop in the relative area of the other two shorter relaxation time peaks (P1 + P2).

3.3. The effect of thermal gelatinisation on the water proton transverse relaxation

The melting transition can also be followed using the CPMG sequence in the packed bed containing water (H_2O). This complements the starch chain dynamics by reporting on the changing microscopic distribution of the water in the granule compartments. The relaxation time distribution also reports indirectly on the dynamic state of the starch chains. This is because the transverse relaxation time of the exchangeable water protons is largely determined by fast chemical exchange with hydroxyl protons on the starch. The more rigid the starch, the shorter the

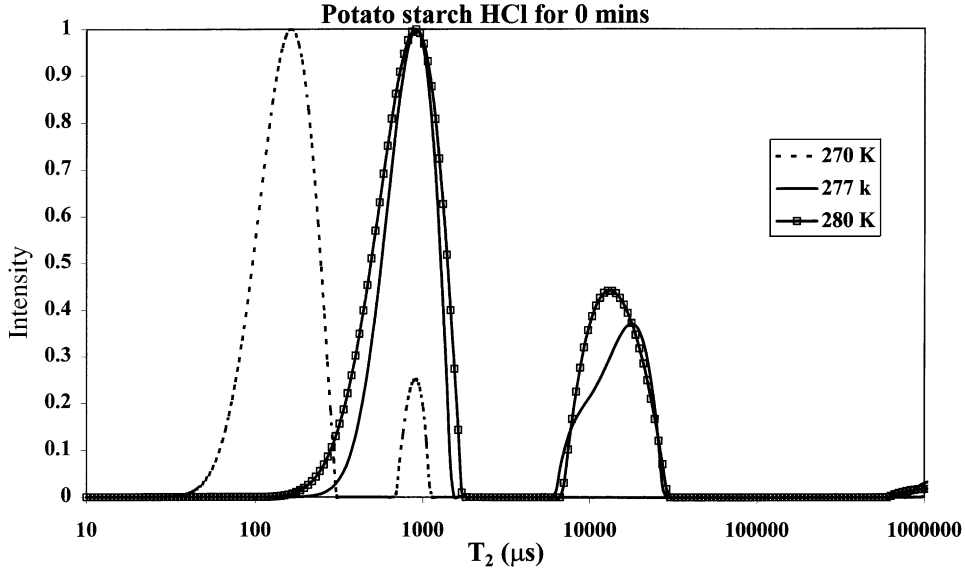

Fig. 7. The distribution of water proton transverse relaxation times measured with the CPMG sequence at the indicated temperatures for a packed bed of native potato starch granules exposed to Lintnerisation for ca. 1 min. The measurements are made on a packed bed in distilled water at neutral pH.

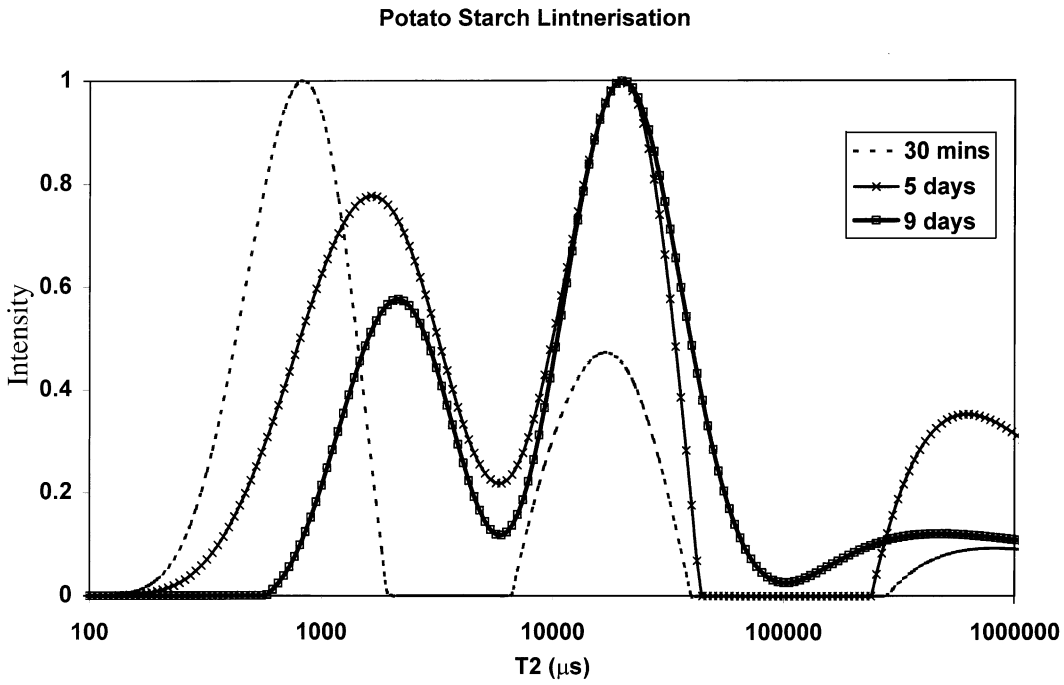

Fig. 8. The distribution of water proton transverse relaxation times measured with the CPMG sequence at 298 K for a packed bed of native potato starch granules exposed to Lintnerisation for the indicated times. The measurements are made on a packed bed in distilled water.

transverse relaxation time of the exchangeable starch hydroxyl protons and therefore of the water (Hills). As a first approximation the transverse relaxation time of the starch hydroxyl protons can be equated to that of the non-exchangeable starch CH proton pool reported in the previous section. It is therefore of interest to see how gelatinisation changes the water proton relaxation spectrum and to compare it with the data in Figs. 2–4. The distribution at 313 K in Fig. 6 shows the same three peaks seen at 300 K in Fig. 1, but as the temperature is raised to 335 K the relative area of the central relaxation time peak at ca. 5 ms corresponding to water inside the granules increases, presumably reflecting the swelling of the granules. Above the melting transition

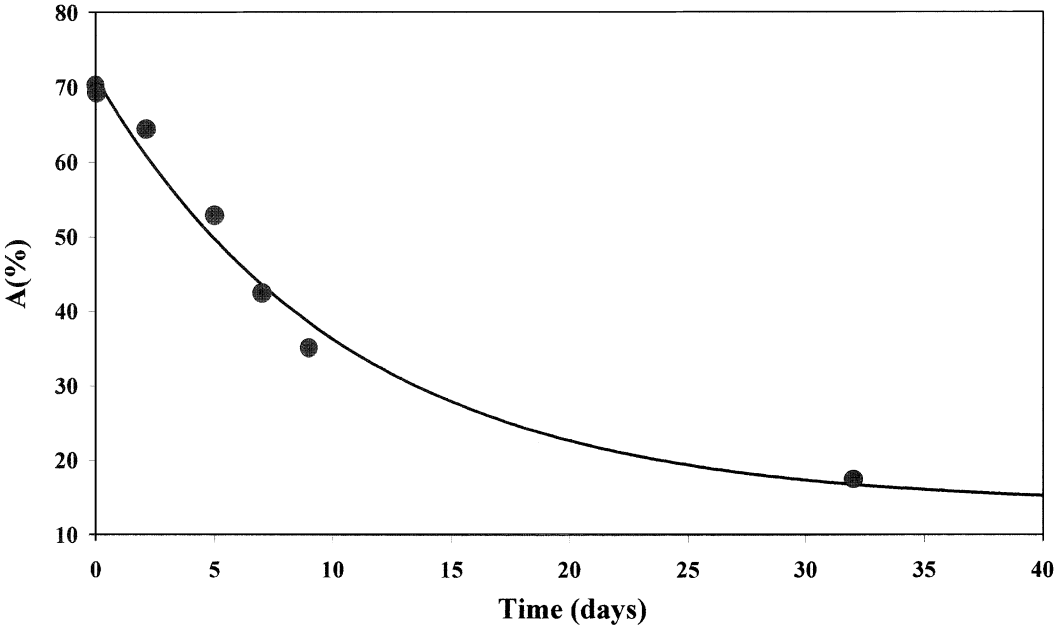

Fig. 9. The decrease in the % area of the lowest relaxation time peak in Fig. 8 with increasing Lintnerisation time. The smooth curve is the best fit exponential decay function.

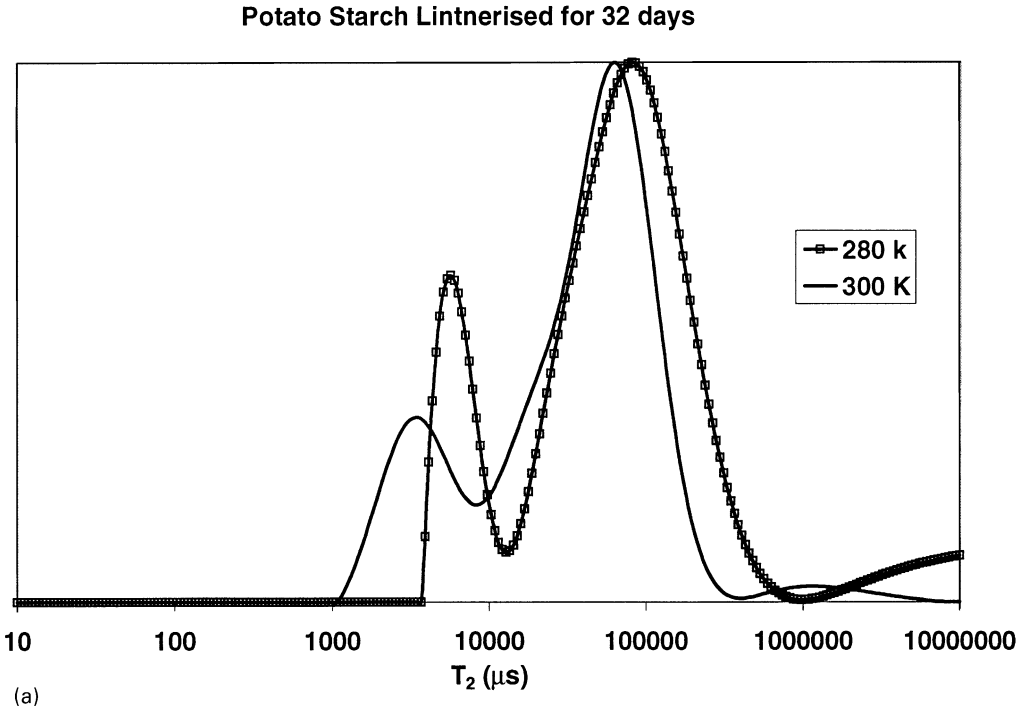

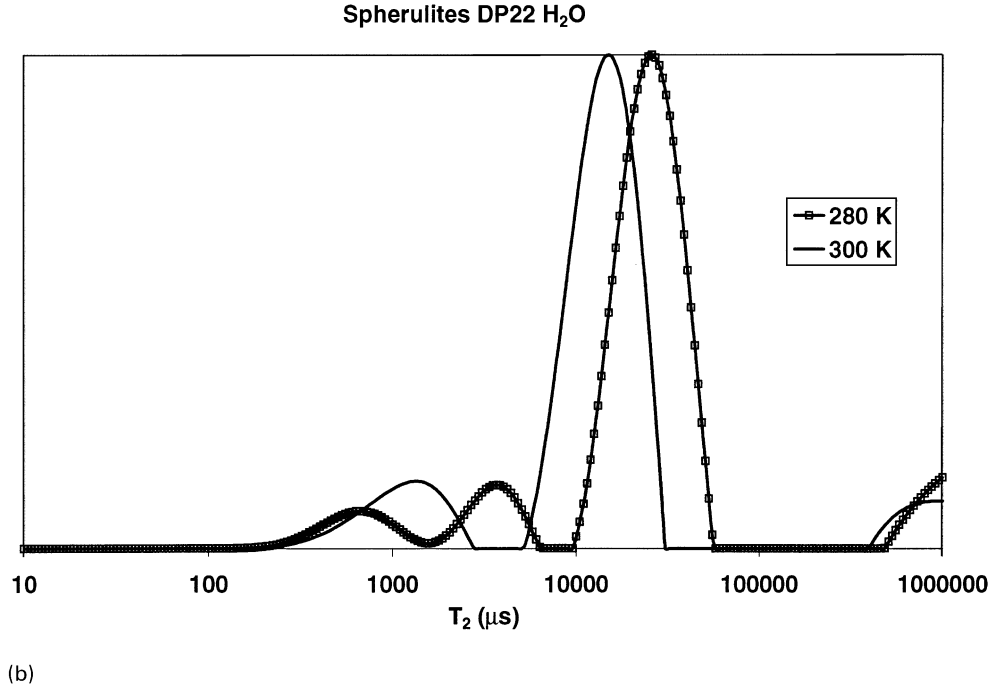

Fig. 10. The distribution of water proton transverse relaxation times measured with the CPMG sequence for (a) A packed bed of native potato starch granules exposed to Lintnerisation for 32 days. (b) Recrystallised Spherulites, DP 22. The measurements are made on a packed bed in distilled water at the indicated temperatures.

temperature of 335 K the peak shifts and then decreases in area as amylose diffuses out of the granule.

When the system is cooled back to 296 K Fig. 4 shows that the main relaxation peak at 1 ms reappears suggesting that the plasticisation of the amylopectin in the B-type crystallites is, to some extent, reversible. However, the three relaxation peaks corresponding to gelled starch do not disappear and are irreversible results of the thermal treatment.

The dramatic changes in the NMR relaxation time spectra

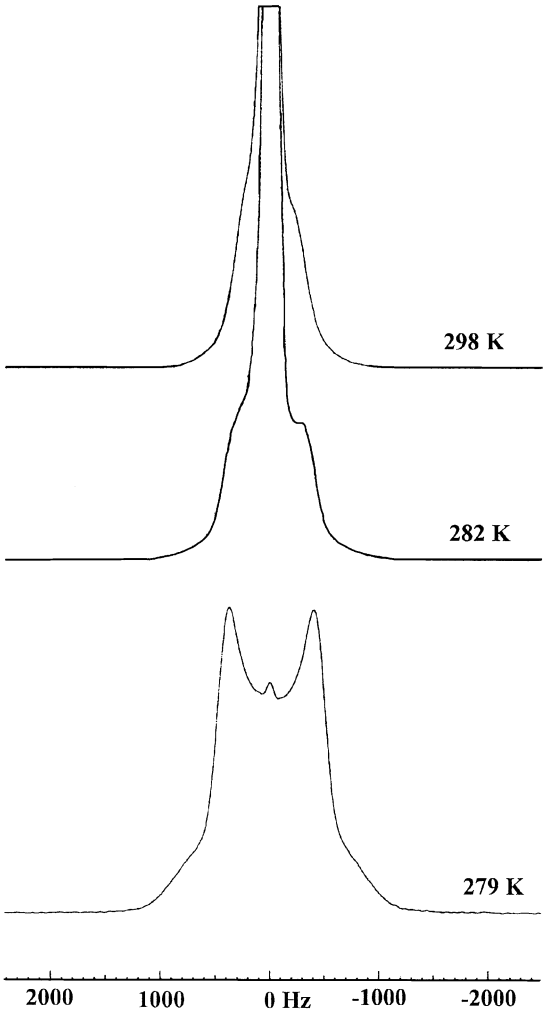

Fig. 11. The wide-line deuterium spectrum measured at the indicated temperatures for a packed bed of potato granules in D_2O after Lintnerisation for 32 days.

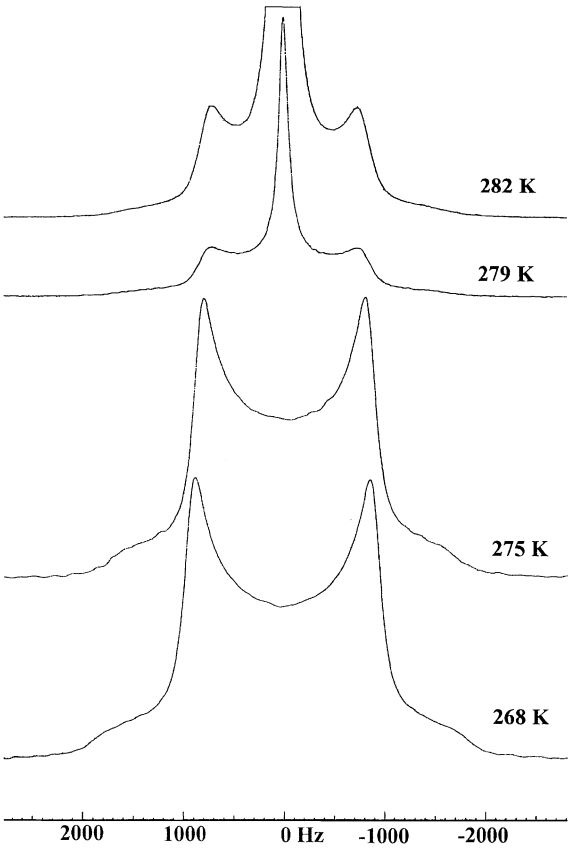

Fig. 12. The wide-line deuterium spectrum measured at the indicated temperatures for a packed bed of Sperulites, DP 22 in D_2O.

caused by gelatinisation and seen in Figs. 2–6 raise the possibility of following the kinetics of gelatinisation in real time. A relaxation time spectrum can be acquired in about 30 s, so that, provided small samples are used to permit rapid thermal equilibration, both equilibrium and non-equilibrium gelatinisation can be compared and monitored as a function of varying water content and for different starch modifications.

3.4. Lintnerisation

If it is true that during the first few days of Lintnerisation acid attacks the amylose in the amorphous growth rings, which is the most accessible starch fraction, then it should cause major changes in the NMR water proton relaxation spectrum and allow the hydrolysis kinetics to be investigated.

Fig. 7 shows the CPMG relaxation time distribution for potato starch that has been Lintnerised for just a minute before being filtered, washed and examined as a water-saturated packed bed at neutral pH. Comparison of the resulting distribution (Fig. 7) with that for untreated starch (Fig. 1) shows that even very brief acid treatment has caused a very rapid and dramatic shift of the longest relaxation time peak at about 80 ms (at temperatures above 273 K) and assigned to water outside the granules, to a shorter relaxation time of about 1 ms. The most likely explanation is the rapid hydrolysis of amylose chains projecting out of the surface of the granule and into the extragranular water. Removal of these chains permits the washed granules to pack more densely and results in a shortening of the relaxation time of the water in the thin film between the granules. The smaller peak at ca. 10 ms therefore arises from water inside the granule.

Fig. 8 shows the water proton transverse relaxation time distribution after 30 min, 5–9 days of exposure to the acid. The most noticeable change is the progressive decrease in the relative area of the peak at about 1 ms relative to the peak at ca. 10 ms and its shift to longer relaxation times. The long relaxation time peak at ca. 1 s arises from supernatant water on top of the granule bed and can be ignored. The changes in area are easy to understand if the acid hydrolysis causes an increase in the relative amount of water inside the granules compared to that outside. This could result either from closer packing or because the hydrolysis causes

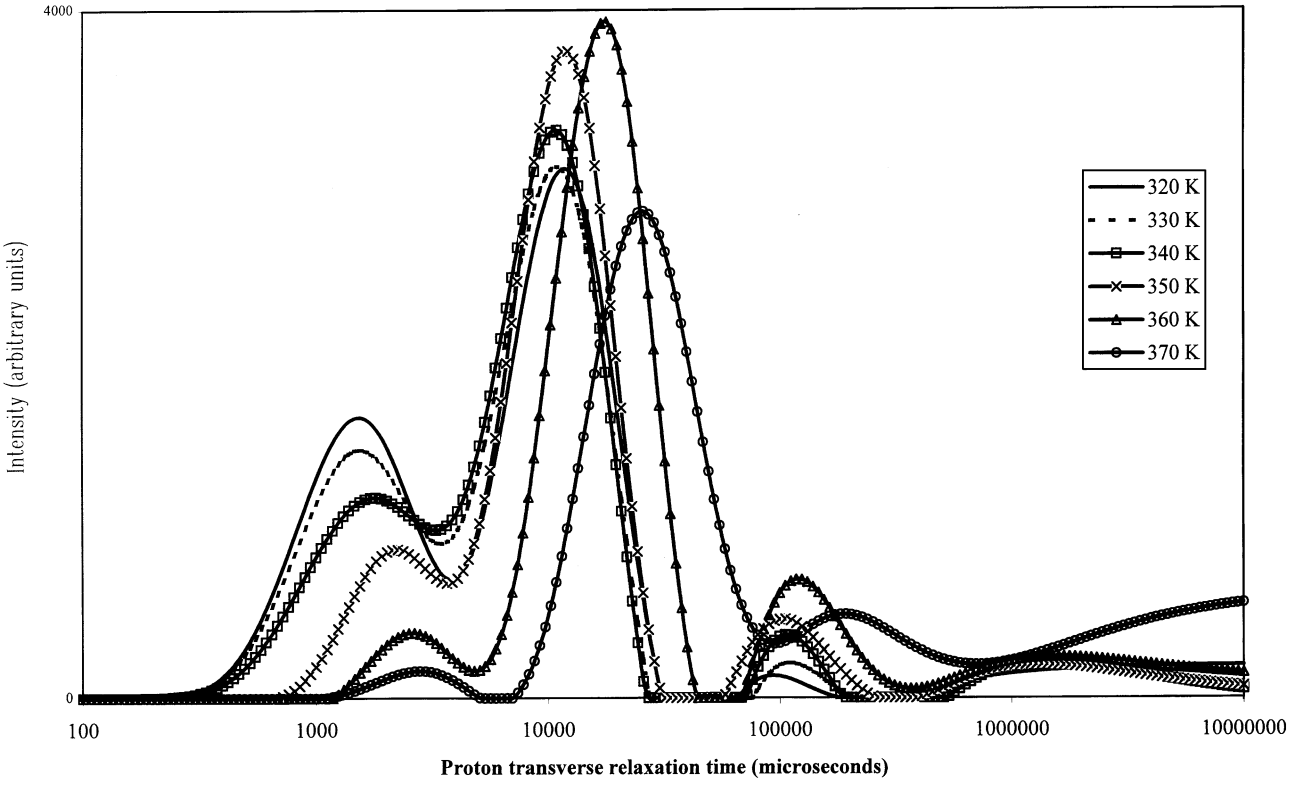

Fig. 13. The effect of gelatinisation on the distribution of water proton transverse relaxation times for a packed bed of potato starch granules that have been Lintnerised for 8 days.

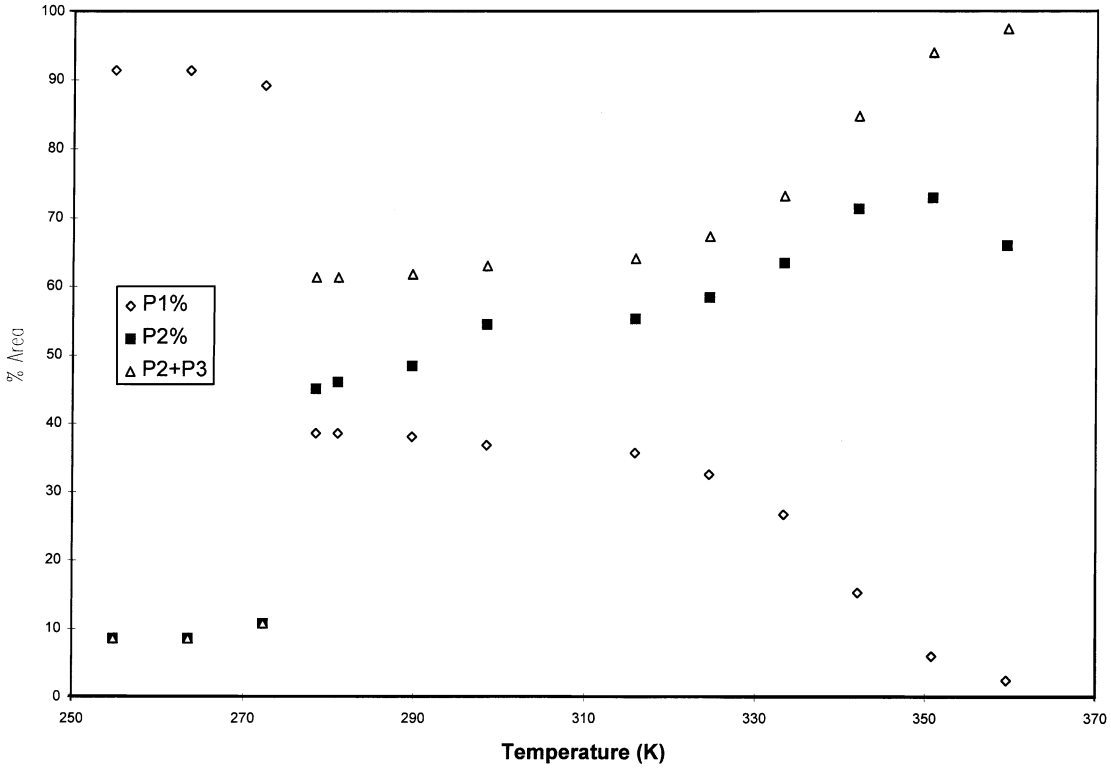

Fig. 14. The temperature dependence of the relative peak areas in Fig. 13. P1 refers to the shorter relaxation time peak at ca. 1 ms. P2 refers to the main longer relaxation time peak.

granule swelling or a combination of both. The shift in the peak at 1 ms to longer relaxation times is harder to explain but could simply reflect the increasing mobility of starch at the periphery of the granules. Because of fast proton exchange between the bulk water and the starch hydroxyl protons this will also increase the relaxation time of the intergranule water. The Lintnerisation kinetics can be followed by plotting the decreasing % area of the shorter relaxation time peak when an exponential decrease in area is observed (see Fig. 9).

After extended periods of hydrolysis the progressive hydrolysis results in a shift in the longest relaxation time peak in Fig. 8, corresponding to water inside the granules, to longer relaxation times as the amylopectin chain mobility increases and the starch concentration inside the granule decreases. Fig. 10a shows the relaxation spectrum after 32 days Lintnerisation where the longest peak is now shifted to 100 ms. It is also interesting to compare the relaxation spectrum in Fig. 10a after 32 days Lintnerisation with that of a sample of a recrystallised Spherullite DP 22. The resemblance of these two systems shows that the granule still retains significant structure despite the extensive hydrolysis. Raising the temperature can be seen to cause slight shifts to shorter relaxation times and a peak broadening. This indicates that there is still some exchange averaging of water between the compartments by diffusion and proton exchange. It is noteworthy that a small room temperature relaxation peak at about 2 ms still exists and this is most probably the residual water in the hexagonal channels of the B-type crystals of amylopectin. This assignment is supported by the observation of an ca. 1 kHz deuterium splitting in the wide line deuterium spectrum of the 32 day residue when water (H_2O) is replaced by D_2O (see Fig. 11). A slightly larger 1.4 kHz splitting is seen in the deuterium spectrum of the D_2O exchanged spherulites which also have the ordered B-type crystallites (Fig. 12).

3.5. Gelatinisation of the Lintnerised starch

Fig. 13 shows the effect of heating the acid treated starch remaining after 8 days of Lintnerisation. The thermal treatment causes a progressive disappearance of the shorter peak at 2 ms and the appearance of longer relaxation time peaks at >100 ms corresponding to amylose gel. If our earlier peak assignments are correct and the peak at 1 ms arises from intergranular water, then the progressive decrease in area presumably results from plasticisation resulting in granule swelling. At the same time, the appearance of new peaks having long relaxation times (>100 ms) presumably corresponds to the formation of dilute amylose gel.

Fig. 14, which plots the relative peak area of the shorter relaxation peak shows that the melting transition temperature is now shifted to slightly higher temperatures, with a mid-point around 340 K and the melting transition appears somewhat more spread-out, with an lower onset temperature of 310 K. This is in contrast to the sharper transitions in the native granule (Figs. 3 and 5) where the onset temperature is about 330 K and the mid-point at ca. 335 K.

4. Discussion

It is clear that relatively straightforward NMR relaxation time measurements offer unique insight into the starch gelatinisation and Lintnerisation processes. While many techniques offer insights into the microstructural changes induced by acid hydrolysis and gelatinisation, NMR relaxometry is unique in providing information on the changing starch chain dynamics and the changing microscopic distribution of water within the granules. The starch chain dynamics clearly reflect a melting transition at 335 K (see, for example, Fig. 3) and this is associated with granule swelling and the removal of amylose from inside the granule. As expected, acid hydrolysis first acts on the surface of the granule, then on the starch in the amorphous growth rings, resulting in an exponential decrease in the relaxation time peak areas and a shift in the melting transition to slightly higher temperatures. Surprisingly, even after 32 days Lintnerisation, there is still a clear splitting in the deuterium spectrum which shows that the B-type amylopectin crystal structure remains largely intact.

Although the NMR relaxation technique is sensitive to quite subtle changes, assigning the various relaxation time peaks to particular proton populations of the amylose, amylopectin and water compartments within the granule remains a major difficulty. Nevertheless, the results pave the way for a number of interesting comparative kinetic studies where the effects of modifying granule structure on the gelatinisation and Lintnerisation kinetics can be explored. This will be the subject of future reports.

Acknowledgements

The authors thank Drs Steve Ring and Vic Morris for helpful discussions and for supplying the recrystallised spherulite samples. Financial support from the BBSRC is gratefully acknowledged.

References

Blanshard, J. M. V. (1987). In T. Galliard, *Starch: properties and potential*, New York: Wiley, chapter 2.

Donald, A. M., Waigh, T. A., Jenkins, P. J., Gidley, M. J., Debet, M., & Smith, M. (1997). In P. J. Frazier, A. M. Donald & P. Richmond, *Starch: structure and functionality*, Cambridge: Royal Society of Chemistry.

Donovan, J. (1979). *Biopolymers*, *18*, 263.

Gallant, D. J., Bouchet, B., & Baldwin, P. M. (1997). *Polymer*, *32*, 177–191.

Hills, B. P. (1992). The proton exchange cross-relaxation model of water relaxation in biopolymer systems. *Molecular Physics, 76*, 489–508.

Hermansson, A.-M., Kidman, S., & Svegmark, K. (1995). In S. E. Harding,

S. E. Hill & J. R. Mitchell, *Biopolymer mixtures*, chapter 12. Nottingham University Press.

Jacobs, H., Eerlingen, R. C., Rousen, N., Colonna, P., & Delcour, J. A. (1998). Acid hydrolysis of native and annealed wheat, potato and pea starches — DSC melting features, and chain length distributions of lintnerised starches. *Carbohydrate Research*, *308*, 359–371.

Jenkins, P. J., & Donald, A. M. (1997). The effect of acid hydrolysis on native starch granule structure. *Starch*, *49*, 262–267.

Jenkins, P. J., & Donald, A. M. (1998). Gelatinisation of starch: a combined SAXS/WAXS/DSC and SANS study. *Carbohydrate Research*, *308*, 133–147.

Morris, V. J. (1990). Starch gelation and retrogradation. *Trends in Food Science and Technology*, *July*, 2–6.

Muhr, A. H., Blanshard, J. M. V., & Bates, D. R. (1984). The effect of Lintnerisation on wheat and potato starch granules. *Carbohydrate Polymers*, *4*, 399–425.

Robin, J. P., Mercier, C., Charbonniere, R., & Guilbot, A. (1974). Lintnerized starches. Gel filtration and enzymatic studies of insoluble residues from prolonged acid treatment of potato starch. *Cereal Chemistry*, *51*, 389–405.

Robin, J. P., Mercier, C., Duprat, F., Charbonniere, R., & Guilbot, A. (1975). Lintnerized starches. Chromatographic and enzymatic studies of insoluble residues from acid hydrolysis of various cereal starches, particularly waxy maize starch. *Starch*, *27*, 36–45.

Tang, H. R., & Hills, B. P. (2000). The distribution of water in native starch granules — a multinuclear NMR study. *Carbohydrate Polymers*, *43*, 375–387.